

A MULTIWAVELENGTH STUDY OF RZ CASSIOPEIAE: THE XMM-NEWTON/VLA CAMPAIGN

M. Audard¹, J. R. Donisan¹, and M. Güdel²

¹Columbia Astrophysics Laboratory, Columbia University, Mail code 5247, 550 West 120th Street, New York, NY 10027, USA

²Paul Scherrer Institut, Villigen & Würenlingen, 5232 Villigen PSI, Switzerland

ABSTRACT

XMM-Newton and the VLA simultaneously observed the eclipsing Algol-type binary RZ Cassiopeiae in August 2003. The secondary eclipse (K3 IV companion behind the A3 V primary) was placed at the center of the 15-hour radio campaign, while the X-ray satellite monitored a full 1.2-day orbital period. We present results of the X-ray and radio campaigns. The X-ray light curve shows significant modulation probably related to rotational modulation and active region evolution, and even small flares. However, the X-ray eclipse is not deep, implying that the coronal X-ray emitting material is spatially extended. The Reflection Grating Spectrometer (RGS) spectrum shows a variety of bright emission lines from Fe, Ne, O, N. A strong [C/N] depletion probably reflects the surface composition of the secondary which fills its Roche lobe and loses material onto the primary. The O VII He-like triplet reflects a low forbidden-to-intercombination ratio; while it generally suggests high electron densities, the ratio is here modified by photoexcitation by the strong UV flux of the primary A3 V star. The radio light curve shows no similarity to the X-ray light curve. The eclipse timings are different, and the radio flux increased while the X-ray flux decreased. The radio spectral slope is shallow ($\alpha = 0 - 1$).

Key words: Stars: activity – Stars: coronae – Stars: individual: RZ Cas – radio: stars – X-rays: stars

1. INTRODUCTION

Direct imaging of stars still remains exceptional, and approximate geometric information on the coronae of stars must be obtained from indirect methods such as image reconstruction from rotational modulation or eclipse mapping. The latter is a powerful means to image the corona of a star when applied to Algol-type systems which are semi-detached binaries composed of a massive early-type star orbiting an evolved late-type star. The latter fills its Roche lobe, hence a gas stream flows from the L1 Lagrange point (Hall 1989). The coronal emission originates exclusively from the late-type companion; therefore, the simultaneous X-ray and radio eclipses at phase 0.5 can constrain the location of the coronal emitting regions and provide powerful information on the co-spatiality of the emission

regions, with important implications for the structure of the outer atmospheres.

In Algol-type systems, the formation of an accretion disk around the primary depends on the location of the binary in the r - q diagram, where r is the radius of the primary in units of the binary separation, and q is the mass ratio of the secondary to the primary (Peters 1989). In brief, short-period Algols, such as our target RZ Cas, tend to populate a region of the r - q diagram where the gas stream directly impacts on the primary while eventually forming a transient accretion disk. Although the presence of circumstellar material has been indirectly inferred from H α difference profiles (Richards et al. 1999), its detection is still elusive in the X-rays. However, cool material can absorb X-rays if located along the line of sight, thus producing an extra column density detectable in X-rays.

We present results of a multiwavelength coordinated campaign on RZ Cas in X-rays with *XMM-Newton* and in radio with the VLA.

2. RZ CASSIOPEIAE

RZ Cas is a nearby ($d = 63.54$ pc) Algol-type binary, consisting of an A3 V primary and a K3 IV secondary with similar radii ($R_1 = 1.67 R_\odot$, $R_2 = 1.94 R_\odot$, $A = 6.77 R_\odot$; Maxted et al. 1994), orbiting with synchronous rotation ($P \approx 1.195$ d; Narusawa et al. 1994). Their masses are, however, different, with $M_1 = 2.2 M_\odot$ and $M_2 = 0.73 M_\odot$. The secondary fills its Roche lobe, and a flow of material falls directly onto the primary (Olson 1982; Richards et al. 1999). The orbital inclination angle ($i = 83.3^\circ$) leads to almost complete eclipses.

Singh et al. (1995) found that RZ Cas displays variable X-ray luminosity, with a spread of an order of magnitude ($\log L_X = 30.36 - 31.18$ erg s⁻¹). They also found that a two-temperature optically thin plasma model was required to fit their *ASCA* and *ROSAT* PSPC data, along with abundances about 0.2 times the solar photospheric values. Their *ROSAT* observations showed significant intensity variations, apparently unrelated to the eclipse, but probably originating from either rotational modulation, flare activity, or inhomogeneous distributions of coronal structures on the secondary. A core-halo structure was proposed from radio data by Umana et al. (1999), whereas Gunn & Brady (2003) observed a radio modulation close to the primary eclipse seemingly correlating with X-rays.

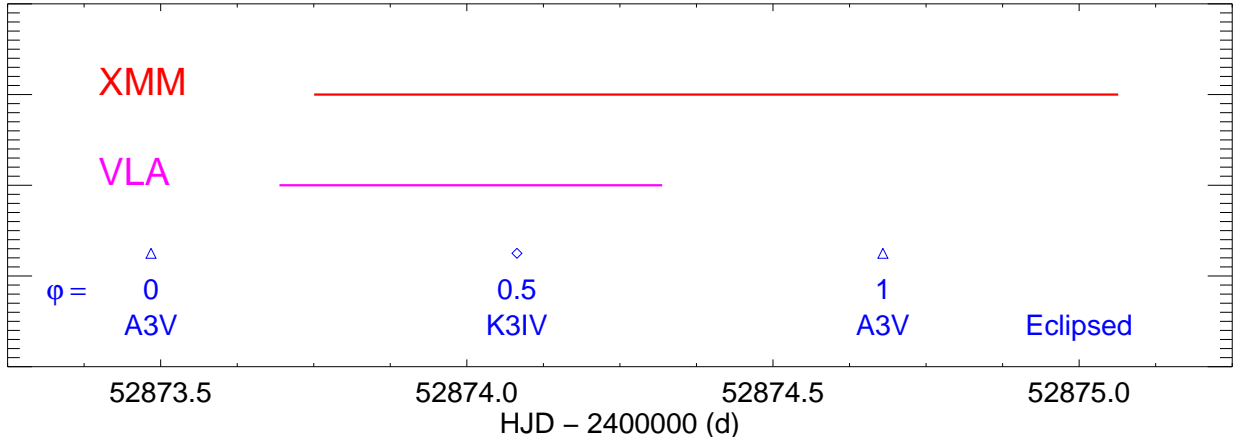


Figure 1. Schematic diagram of the coordinated campaign with XMM-Newton and the VLA. The horizontal lines show the observation time ranges for each observatory (30.55 hrs with XMM-Newton, 15 hrs with VLA). The orbital phases are shown in the lower part, with the eclipsed star indicated.

3. OBSERVATIONS AND DATA REDUCTION

XMM-Newton observed RZ Cas for 110 ks from August 22 (5h23m54s UT) to August 23, 2003 (13h41m23s UT), whereas the VLA observed on August 22, 2003 from 4h41m20s UT to 19h38m30s UT. The VLA was in A-array configuration, and we observed alternatively in the C (6.1 cm) and X (3.55 cm) bands, with 0137+331 (3C 48) as flux calibrator and 0228+673 as phase calibrator. Figure 1 shows a diagram of the coordinated observations.

The X-ray data were reduced with the XMM-Newton SAS software (version 6) using standard procedures. The radio data were reduced with AIPS (December 31, 2003 version) using standard techniques. The phases before 9h UT and after 16h UT were significantly degraded due to strong cumuloform clouds. No reliable solutions could be found during these periods (see shaded regions in Fig. 2). We used different techniques to obtain the radio light curves in both bands and to check their consistency.

4. LIGHT CURVES

Figure 2 shows the X-ray pn light curve for events from 0.25 to 8 keV (panel a) and a light curve of a hardness ratio (panel b) defined here as the ratio between the count rates in the hard band (1.5 – 8 keV) and the soft band (0.25 – 1.5 keV). The X-ray eclipse is almost absent, with a local X-ray minimum about an hour *after* the optical eclipse of the K3 subgiant. The light curve modulation suggests, instead, the presence of extended X-ray sources which are not significantly eclipsed and are rotationally modulated (e.g., in particular in the phase range $\varphi = 0.25-0.75$). It could also reflect the evolution of active regions in RZ Cas. A flare was observed at $\varphi = 0$, i.e., at the time of the eclipse of the primary A3 V star. However, the synchronous rotation of the stars does not suggest that $\varphi = 0$ should be a special orbital phase for flares. We

found also that RZ Cas significantly became significantly and steadily hotter in the second half of the observation, as shown in the hardness ratio light curve. No obvious flare can explain such hardening, therefore we hypothesize that hot, active regions rose in this time span, probably due to some reconfiguration of the magnetic topology in RZ Cas.

The radio light curves in X and C bands are also shown in Figure 2 in panels (c) and (d), respectively. A similar flux level was observed in both frequencies. Panel (e) of Fig. 2 shows a light curve of the spectral index α (assuming a power law for the radio spectrum, i.e., $S \sim \nu^{-\alpha}$). The shaded time ranges in the radio light curves correspond to time spans when an accurate calibration could not be obtained. The index α appears to be shallow ($\alpha = 0 - 1$) between 4.9 GHz and 8.4 GHz. This is consistent with the core-halo model proposed by Umama et al. (1999) for RZ Cas. The radio light curves show a steady flux increase, an a possible shallow eclipse is observed about 1.5 hours *before* the optical secondary eclipse. The spectral index α possibly flattens during the radio eclipse.

The marked difference in i) eclipse timing, and ii) in flux modulation in the X-rays and radio strongly suggests that the emitting sources are not co-spatial, at least during this coordinated campaign. This does not support the findings of Gunn & Brady (2003). In addition, the shallow eclipses preclude compact sources in both wavelength regimes. Furthermore, the absence of eclipse at phase $\varphi = 0$ indicates that the primary A-type star does not emit significant X-rays. Finally, the lack of significant eclipses at both primary and secondary eclipses precludes intrabinary (or accretion spot) X-ray and radio emissions in RZ Cas. Instead, the light curves imply rotational modulation of extended sources and active regions rise in the second half of the X-ray observation.

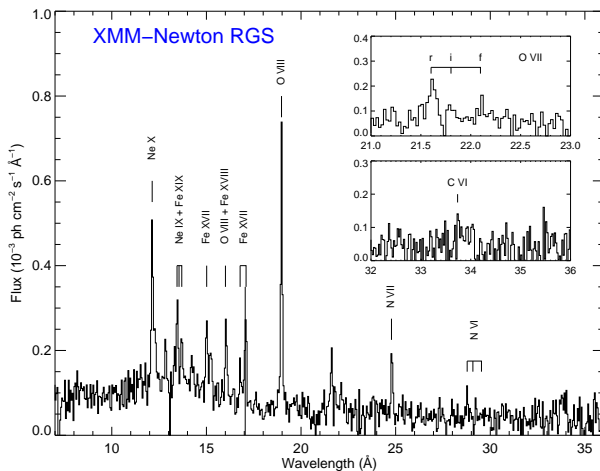


Figure 3. *XMM-Newton* RGS fluxed spectrum of RZ Cas. Major emission lines are labeled. Notice the strong N VII Ly α line and weak C VI Ly α line, a signature of CNO-processed material.

5. X-RAY SPECTRA

Figure 3 shows the average *XMM-Newton* RGS spectrum of RZ Cas. Strong emission lines of O VIII, Ne X, Ne IX, and several Fe L-shell lines can be observed on top of an underlying continuum. The high Ne X/Ne IX and O VIII/O VII ratios indicate a dominant hot plasma in RZ Cas’s corona. The faint O VII triplet suggests a high intercombination-to-forbidden line ratio, albeit with a large error bar. Although such a ratio could be indicative of a high-density ($n_e = 10^9 - 10^{11} \text{ cm}^{-3}$) plasma, it is in fact artificial and due to the strong UV field from the early-type primary (see Ness et al. 2002). The poor signal-to-noise ratio in the triplet prevented us from obtaining a phase-dependent line ratio, which would have confirmed the influence of the UV field (minimal close to $\varphi = 0.5$, maximal close to $\varphi = 0$).

We performed a multi- T fit of the RZ Cas data using both MOS spectra in the 1.55 – 18 Å range and both RGS spectra above 8 Å. We also discarded several wavelength ranges of the RGS data to avoid bias from poorly known L-shell lines of low-Z ions (see Audard et al. 2003). A 4- T model fits the data adequately ($\chi^2 = 1602$ for 1202 d.o.f.), with $T_1 = 3.6^{+0.8}_{-0.6}$ MK, $T_2 = 7.6^{+1.3}_{-5.8}$ MK, $T_3 = 11.6^{+14.2}_{-2.8}$ MK, $T_4 = 25.5^{+3.5}_{-1.6}$ MK, $\log \text{EM}_1 = 52.11^{+0.23}_{-0.25} \text{ cm}^{-3}$, $\log \text{EM}_2 = 52.64^{+0.22}_{-1.53} \text{ cm}^{-3}$, $\log \text{EM}_3 = 52.50^{+0.11}_{-0.55} \text{ cm}^{-3}$, $\log \text{EM}_4 = 53.03^{+0.05}_{-0.21} \text{ cm}^{-3}$. Coronal abundances (relative to the solar photospheric abundances; Grevesse & Sauval 1998) are C = $0.15^{+0.15}_{-0.15}$, N = $0.85^{+0.36}_{-0.32}$, O = $0.38^{+0.06}_{-0.05}$, Ne = $0.97^{+0.12}_{-0.11}$, Mg = $0.68^{+0.08}_{-0.07}$, Si = $0.31^{+0.05}_{-0.05}$, S = $0.15^{+0.06}_{-0.06}$, Ar = $0.27^{+0.33}_{-0.27}$, Ca = $0.60^{+0.34}_{-0.33}$, Fe = $0.37^{+0.04}_{-0.04}$. All quoted uncertainties are 90 % confidence ranges ($\Delta\chi^2 = 2.71$). The high N/C abundance ratio is a strong signature of CNO cycle processed material. This has been observed in Algol (Drake 2003) and in the rapidly rotating giant star YY Men (Audard et al. 2004).

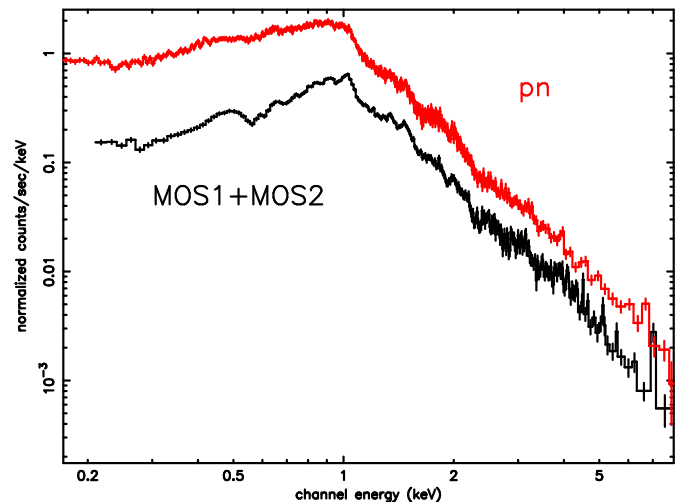


Figure 4. *XMM-Newton* EPIC average spectra of RZ Cas.

We also performed time-dependent spectroscopy using the EPIC MOS spectra only. We observed no significant variation in abundances. However, consistently with the hardness ratio light curve (Fig. 2), we obtained slightly hotter plasma in the second half of the observation, in particular in the last high-flux time segment. We also observed no variation in the spectral slope at low energies, implying that photoelectric absorption (e.g., due to the accretion disk near $\varphi = 0$) remained constant and was consistent with interstellar absorption.

ACKNOWLEDGEMENTS

Based on observations obtained with *XMM-Newton*, an ESA science mission with instruments and contributions directly funded by ESA Member States and NASA. The NRAO is a facility of the NSF operated under cooperative agreement by Associated Universities, Inc. M. A. and J. R. D. acknowledge support from NASA grant NNG04GA42G, and M. G. from the Swiss NSF (grant 20-66875.01).

REFERENCES

- Audard, M., Güdel, M., Sres, A., et al. 2003, *A&A*, 398, 1137
 Audard, M., Telleschi, A., Güdel, M., et al. 2004, *ApJ*, in press
 Drake, J. J. 2003, *ApJ*, 594, 496
 Grevesse, N., & Sauval, A. J. 1998, *Space Science Reviews*, 85, 161
 Gunn, A. G., & Brady, P. A. 2003, *MNRAS*, 346, 337
 Hall, D. S. 1989, *Space Sci. Rev.*, 50, 219
 Maxted, P. F. L., Hill, G., & Hilditch, R. W. 1994, *A&A*, 282, 821
 Natta, A., & Smeets, Y., Nakamura, Y., & Yamasaki, A. 1994, *AJ*, 107, 1141
 Ness, J.-U., Schmitt, J. H. M. M., Burwitz, V., et al. 2002, *A&A*, 387, 1032
 Olson, E. C. 1982, *ApJ*, 259, 702
 Peters 1989, *Space Sci. Rev.*, 50, 9
 Richards, M. T. & Albright, G. E. 1999, *ApJS*, 123, 537
 Singh, K. P., Drake, S. A., & White, N. E. 1995, *ApJ*, 445, 840
 Umana, G., Leto, P., Triglio, C., Hjellming, R. M., & Catalano, S. 1999, *A&A*, 342, 709

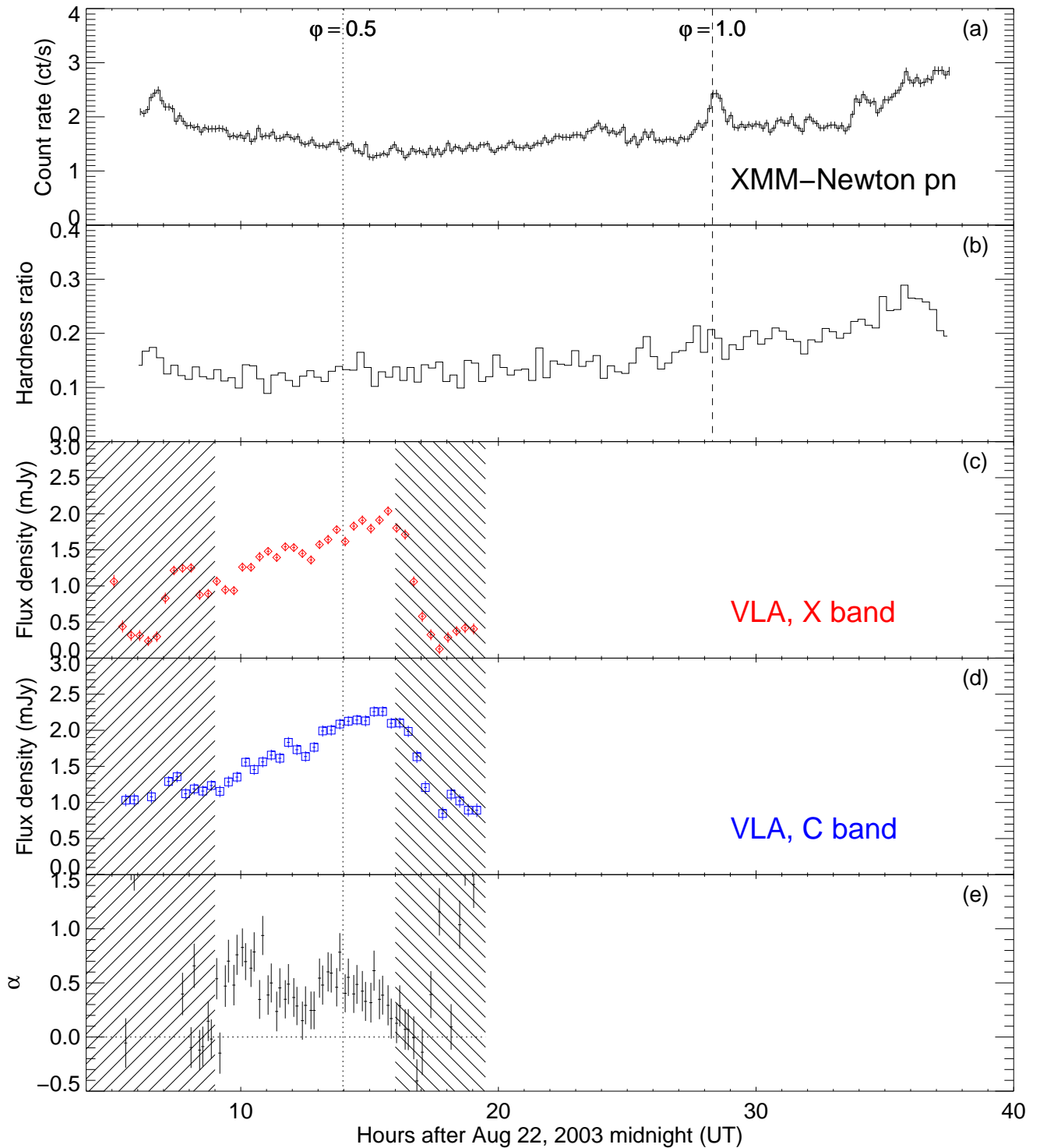


Figure 2. (a) XMM-Newton pn light curve in the 0.25 – 8 keV range, and (b) its hardness ratio for a energy separation at 1.5 keV. Although the ratio does not change significantly during the eclipse, it consistently increases after phase 0.5, which is confirmed by higher plasma temperatures in the later time ranges of the observation. The radio VLA light curves in the X (c) and C (d) bands are also shown. The spectral index α (assuming a power-law shape $S \sim \nu^{-\alpha}$) is shown in the panel (e). A shallow index is observed throughout the observation, consistently with the core-halo model. A possible flattening during the secondary eclipse in the radio is observed. The shallow eclipses observed in both regimes occur, however, at different times.